Patterned Redox Arrays of Polyarylamines II. Growth of Thin Films and Their Electrochemical Behavior

Kye-Young Kim, Joel D. Hassenzahl, Trent D. Selby, Greg J. Szulczewski,* and Silas C. Blackstock*

Department of Chemistry, The University of Alabama, Tuscaloosa, Alabama 35487-0336

Received September 12, 2001. Revised Manuscript Received December 28, 2001

Thin films of tetra-*p*-anisyl-*p*-phenylenediamine, **1**, and *p*-phenylenediamine (PD) with four pendent diarylamino (AA) groups (4AA/PD, **3**) are prepared by vapor deposition under high vacuum. Film growth is studied by atomic force microscopy on mica surfaces. The thin films of **1** and **3** grow very differently. Arylamine **1** grows by a Volmer−Weber type mechanism while **3** grows by a Stranski−Krastanov-type mechanism. The films are amorphous as deposited but convert into crystalline phases upon thermal annealing. Cyclic voltammetry of the films on indium tin oxide coated glass electrodes indicates that the crystalline phase of **1** is oxidized at a higher potential than its amorphous phase. Controlled potential coulometry on 100 nm films shows that oxidation of the core PD group of the shell/core structure **3** is much slower than oxidation of the PD group of **1** in the film state, suggesting that oxidation of the higher $E°'$ arylamino (AA) shell of **3** may be required for bulk charging of its film. The ability of the peripheral AA groups of **3** to electrochemically shield its core PD group is a unique electronic feature derived from the shell/core patterned architecture of this redox-gradient array.

Introduction

The previous paper[1] in this two-part series reports the preparation and solution redox behavior of an arylated *p*-phenylenediamine (PD) structure (**1**) and its arylamino (AA) derivatives (2AA/PD, **2** and 4AA/PD, **3**). The latter structures are small, mixed redox arrays which contain linear and shell/core potential gradients, respectively, within the array. The potential gradient is estimated to be ∼0.2 V in these systems.[1] In this manuscript, studies of film growth and characterization of **1**−**3** are presented along with a study of the film electrochemistry on indium tin oxide (ITO) coated glass substrates.

Arylamines are an important class of molecules used in the fabrication of organic-based electronic and opto-electronic devices.[2,3] Film growth of these compounds is of practical importance to their processability and function. Low molecular weight arylamines (<1000 amu) can form pinhole-free amorphous films with good morphological, thermal, and chemical stability by spin-coating or by vacuum vapor deposition.[4−7] We have previously reported the successful vapor deposition of several higher molecular weight (1000−3000 amu) polyarylamino molecules to prepare thin films.[8] In this

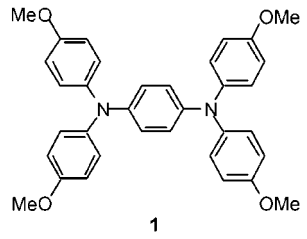

1

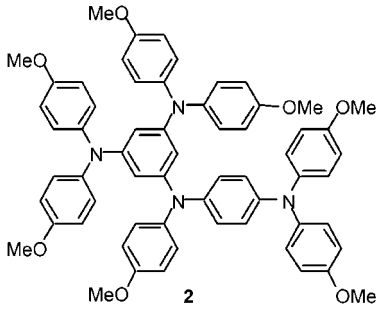

2

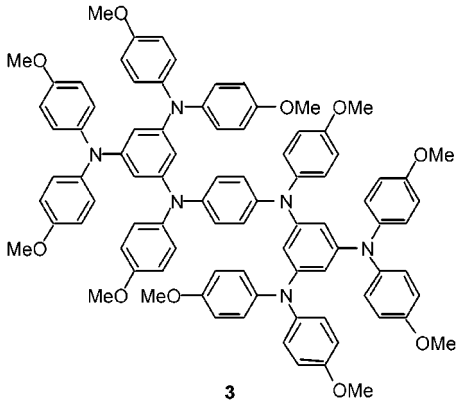

3

* To whom correspondence should be addressed.

(1) Selby, T. D.; Kim, K.-Y.; Blackstock, S. C. *Chem. Mater.* **2002**, *14*, 1685.
(2) Shirota, Y. *J. Mater. Chem.* **2000**, *10*, 1.
(3) Forrest, S. R. *Chem. Rev.* **1997**, *97*, 1793.
(4) Thelakkat, M.; Schmidt, H. W. *Adv. Mater.* **1998**, *10*, 219.
(5) Katsuma, K.; Shirota, Y. *Adv. Mater.* **1998**, *10*, 223.
(6) Shirota, Y.; Kuwabara, Y.; Inada, H.; Wakimoto, T.; Nakada, H.; Yonemoto, Y.; Kawami,; S. Imai, K. *Appl. Phys. Lett.* **1994**, *65*, 807.
(7) Adachi, C.; Nagai, K.; Tamoto N. *Appl. Phys. Lett.* **1995**, *66*, 2679.

10.1021/cm0106771 CCC: $22.00 © 2002 American Chemical Society
Published on Web 03/13/2002

Table 1. Phase Transition Temperatures for 1−3 by DSC

thermal property	1	2	3[a]
T_g (°C)	42	78	97
T_c (°C)	98	*b*	162
T_m (°C)	167	122	272

[a] Reference 8. [b] Not observed.

study, we report on the electrochemical behavior of thin films of newly synthesized redox-gradient polyarylamines[1] and demonstrate the unique charging response of such molecules by comparing the redox behaviors of monomer (**1**), trimer (**2**), and shell/core pentamer (**3**) structures in the film state. In addition, we use atomic force microscopy (AFM) to monitor film growth and thermally induced morphological changes for **1** and **3**.

Experimental Section

Materials and Equipment. Differential scanning calorimetry (DSC) was performed using a TA Instruments model 2920 calorimeter with a nitrogen flow of 40 mL min^{-1} and a heating rate of 10 °C min^{-1}. The crystallization (T_c) and melting (T_m) temperatures are recorded as peak maxima, and the glass transition temperature (T_g) is reported as a midpoint value. Vapor deposition was performed in a high-vacuum chamber with a base pressure of $\sim 2 \times 10^{-7}$ Torr. Typically 10−20 mg of pure compound was placed in an alumina-coated tungsten boat and resistively heated above the melting point of the compound. Films were grown on mica (Ted Pella) and ITO substrates (Corning). ITO glass was cleaned by sonication in detergent followed by rinsing with water, hot trichloroethylene, acetone, and ethanol. The mica was cleaved with double-sided tape and used immediately. The film growth rate ($\sim$0.5 Å sec^{-1}) was monitored by a quartz crystal microbalance (QCM), and the pressure during the deposition was $< 5 \times 10^{-7}$ Torr. After deposition, samples were removed from the chamber under dry, high purity nitrogen and immediately characterized. The purity of the film was verified by dissolving it off the substrate with an appropriate organic solvent and comparing the NMR spectra to the synthesized material. AFM of the vapor-deposited films was performed using a Digital Instruments Dimension 3000 with a Nanoscope III controller. All images were acquired in tapping mode using silicon-etched tips. Scan rates were typically 1−2 Hz with 512 × 512 pixel resolution employed to capture the image. The images were corrected only for long-range flatness.

Cyclic voltammetry (CV) and controlled potential coulometry (CPC) were performed on a PAR 273 electrochemical potentiostat (EG&G Instruments). A three-electrode cell was assembled in a flat-bottomed dish (70 mm diameter × 50 mm height) with an ITO glass working electrode (20 mm × 20 mm), a Pt wire counter electrode, and a saturated calomel electrode (SCE) reference electrode. Films on ITO glass were deposited through contact masks with an aperture to produce a layer of known area on the ITO working electrode. As a result, the films could be dissolved off the ITO and molecular concentration quantified by UV−vis spectrometry. A 0.1 M aqueous solution of $NaClO_4$ was used as supporting electrolyte. A capacitor (0.1 μF), connected between the reference electrode and counter electrode, was used to reduce background noise. All potentials cited below are in V vs SCE and all CV scan rates are 50 mV s^{-1}.

Results and Discussion

The thermal properties of bulk **1**−**3** have been evaluated by DSC and the results are summarized in Table 1. Compound **1** and **3** are isolated as crystalline solids,

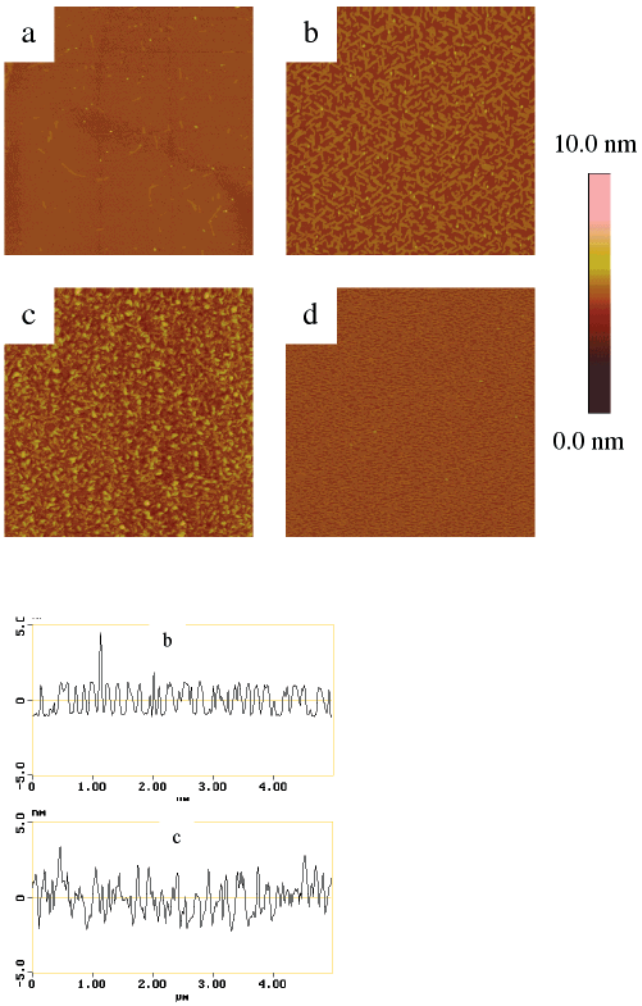

Figure 1. AFM images (5 × 5 μm) of **3** vapor deposited on mica: (a) <1 nm, (b) 1 nm, (c) 2 nm, and (d) 4 nm films and representative line scan for (b) and (c).

but, to date, we have been unable to crystallize compound **2**. Data reported in Table 1 were obtained after an initial melting/cooling cycle. It is evident that all the compounds form molecular glasses upon cooling from the melt and that T_g increases with molecular weight in this series.

Film growth by vapor deposition was studied on a mica surface due to its intrinsic flatness. AFM images were obtained for different film thicknesses of arylamines **1** and **3**. Film "thickness" is calculated from accumulated mass recorded by a QCM (assuming a molecular density of 0.7 g/cm^3 and uniform film formation). A series of AFM images for **3** are shown in Figure 1.

In <1 and 1 nm films, elongated cylindrical islands are observed. In the 1 nm film, the average cylinder length and width are 163 and 74 nm, respectively. Line scans reveal a uniform island height of $\sim$2 nm. A molecular mechanics calculation[9] of the equilibrium geometry of **3** predicts a dumbbell-like shape with pseudoaxial symmetry ($\sim$1.3 × 1.8 nm). Consequently, the line scans suggest that many, if not most, of the molecules are standing on end within the islands. A few

(8) Szulczewski, G. J.; Selby, T. D.; Kim, K.-Y.; Hassenzahl, J.; Blackstock, S. C. *J. Vac. Sci. Technol., A* **2000**, *18*, 1875.

(9) A molecular mechanics minimization of **3** was done using the SYBYL routine (force field developed by Tripos, Inc.) in MacSpartan (Wave function Inc.).

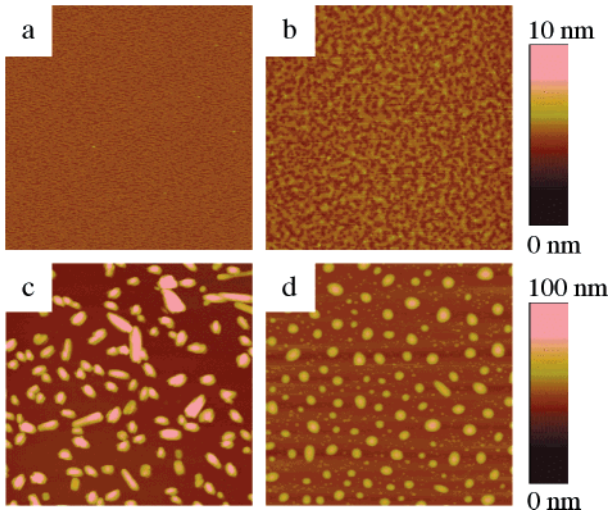

Figure 2. AFM images (5 × 5 μm) of a 4 nm film of **3** on mica: (a) as-deposited, (b) annealed to 110 °C, (c) annealed to 200 °C, and (d) annealed to 300 °C.

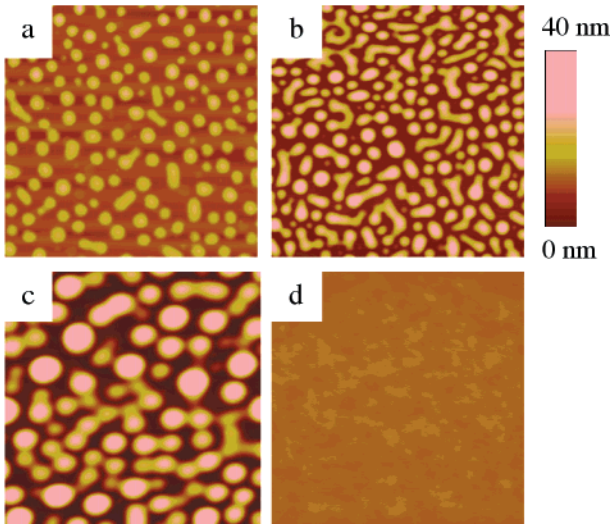

Figure 3. AFM images (5 × 5 μm) of **1** vapor deposited on mica: (a) 1 nm, (b) 4 nm, (c) 10 nm, and (d) 100 nm films.

islands are about twice this height, indicating the onset of 3-D island growth. However, most islands appear to be one molecule high, and the mica surface is about 50% covered. In a 2 nm film of **3**, complete monolayer formation is possible but not observed. Line scans through the 2 nm films show that 3-D islands form prior to complete surface coverage (Figure 1c). In a 4 nm film, the AFM image indicates a smooth topography and the mica is apparently covered. AFM images of films of thickness greater than 10 nm look similar to those of the 4 nm film, so we conclude that after the polar mica surface is covered, film growth occurs in a layer-by-layer fashion (i.e.,Volmer−Weber mechanism).[10]

Thermal annealing of the 4 nm films of **3** on mica was performed to determine the effects of phase change on the thin film morphology. The vapor-deposited film was heated in a vacuum oven (∼10 mTorr) above T_g, T_c, and T_m, each time for 90 min. The sample was cooled to room temperature after each annealing cycle, and an AFM image was recorded (Figure 2). Heating the film to 110 °C shows only a slight roughening of the film, but annealing the sample to 200 °C causes a major change in film morphology, with the formation of large microstructures of **3**, assigned as crystallites.[11] Further heating of the sample to 300 °C results in formation of microglobules, apparently derived from melting/glassing of the crystallites. Thus, we assign these thermally induced morphology changes in the film to softening, microcrystallization, and crystallite melting at 110, 200, and 300 °C, respectively. We conclude that the structural changes in the ultrathin film of **3** on mica, as observed by AFM, are consistent with the thermal transitions observed for bulk **3** by DSC.

Film growth of **1** on mica is dramatically different than that of **3**. AFM images of 1, 4, 10, and 100 nm films of **1** are shown in Figure 3. The images at low coverage (<10 nm) indicate that **1** does not wet the mica surface (i.e., Stranski−Krastanov growth mechanism).[10] We suspect the different film morphologies of **3** and **1** are related mainly to molecular size and thermal property differences of these otherwise similar compounds. The smaller surface area-to-volume ratio of **3** may allow it to better tolerate (and better wet) the polar mica surface than does **1**. Furthermore, the large kinetic energy available to **1** upon impact at the mica surface, combined with its lower T_g, will facilitate its agglomeration into island structures, to the exclusion of surface coverage. In addition, it is possible that the T_g value for thin films of **1** may be lower than that observed for the bulk sample.[12] Once sufficient material has been deposited to finally cover the mica surface, then the film of **1** becomes very smooth (Figure 3d).

When 100 nm vapor-deposited films of **1** on mica or ITO glass are annealed above T_c, there is a visible change in the appearance of the film. Inspection under a polarizing microscope and by AFM revealed that the annealed films contained both crystal and amorphous domains. Unlike films of **3**, the thin films of **1** proved difficult to crystallize quantitatively by annealing, although thicker spin-coated films of **1** did show essentially quantitative crystallization as judged by polarized light microscopy and by electrochemical analysis (vide infra).

Cyclic voltammetry (CV) of **1** was measured on vapor-deposited and spin-coated thin films on ITO glass. Figure 4 shows voltammograms of a 10 nm vapor-deposited and annealed film (110 °C, 1 h). The as-deposited film exhibits oxidation waves at +0.37 and +0.70 V. On the basis of the solution CV for **1**, these peaks are assigned to the first and second oxidation potentials, respectively.[1] Annealing the vapor-deposited film above T_c yields an additional oxidation wave at +0.48 V. As-deposited spin-coated films of **1** show two oxidation peaks in the 0.3−0.5 V range (Figure 5). Annealing the spin-coated sample above T_c causes the peak at 0.36 V to disappear. These results suggest the

(10) Attard, G.; Barnes, C. *Surfaces*; Oxford Press: Oxford, 1998.

(11) In a separate experiment, we verified the crystallinity by X-ray powder diffraction. A 0.5 μm film of **3** was vapor deposited on a polycrystalline 200 nm Au film. XRD of the as-deposited films displays only the Bragg peaks for Au. However, after annealing the film above T_c, a new set of Bragg peaks appeared. The crystal structure will be reported in a future manuscript.

(12) Forrest, J. A.; Jones, R. A. L. The Glass Transition and Relaxation Dynamics in Thin Polymer Films. *In Polymer Surfaces, Interfaces, and Thin Films*; Kumar, K., Ed.; World Scientific: Singapore, 2000.

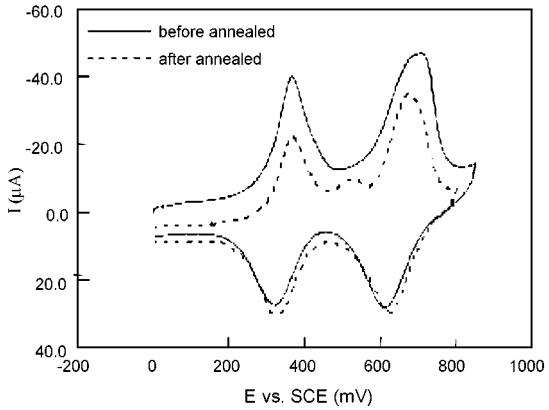

Figure 4. CV of 10 nm vapor-deposited film of **1** on ITO.

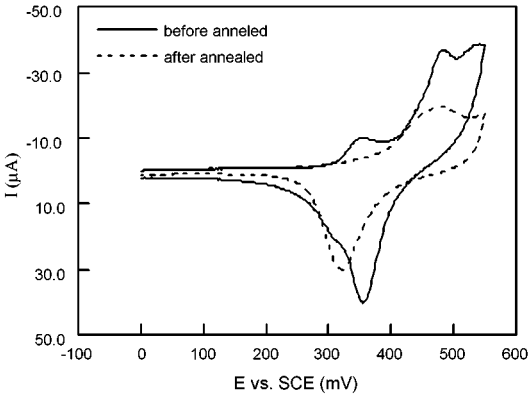

Figure 5. CV of spin-coated film (∼10 nm) of **1** on ITO.

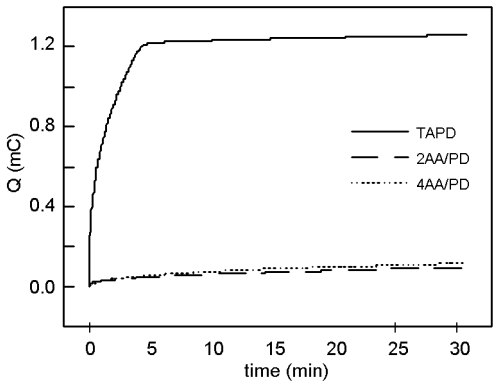

Figure 6. CPC on 100 nm films on ITO held at 0.55 V.

assignment of film oxidation potentials at +0.37 and +0.48 V to neutral/cation conversions of the amorphous and crystalline phases of **1,** respectively.

CV traces of **3** films on ITO glass are not well behaved and are difficult to interpret. Typically, no oxidation current is observed below 0.6 V, and the films generally do not conduct well at low potentials. We suspect that, in films of **3**, intramolecular core charge trapping inhibits conduction, producing poor film CV response compared to what is observed in solution for **3** or in film/solution for **1**.

CPC performed at 0.55 V on 100 nm vapor-deposited films (1.3 cm^2) of **1**, **2**, and **3** on ITO glass gave charging profiles as shown in Figure 6. In replicate experiments, several as-deposited 100 nm films (of each arylamine) were dissolved and analyzed by UV−vis spectrometry to determine the mole composition of the films. Thus, the number of electrons passed per molecule (or per PD group) after 30 min of charging at 0.55 V could be determined and were calculated to be 1.0, 0.12, and 0.25 for **1**−**3**, respectively. These data clearly illustrate the difference in film charging rates for these three cases, which we attribute to poor conductivity in films of **2** and **3** due to their redox gradients, compared to the nongradient case, **1**. In solution, **1**−**3** all show well-behaved CV waveforms with PD group oxidation at $E^{o\prime}(1)$ values of 0.46−0.49 V.[1]

It is evident from the CPC data that the redox gradient in **3** (and in **2**) inhibits bulk charging *in the film state*, even though the applied potential is greater than the solution-derived $E^{o\prime}$ value. In contrast, quantitative oxidation of the film **1** (i.e., one electron removed per molecule) occurs effectively at 0.55 V and is accompanied by green coloration of the film. The formation of pure $\mathbf{1}^{+\bullet}ClO_4^-$ during film charging has been independently verified by dissolving the charged film from the ITO electrode and analyzing the resulting solution by electron spin resonance and optical spectroscopy, with comparison to authentic samples. Neither **2** films nor **3** films give coloration (as would be expected for cation formation) during exposure to 0.55 V CPC conditions. However, charging and coloration does occur at potentials ≥0.6 and ≥0.70 V for **2** and **3**, respectively.

Further experiments are underway to explore the oxidation of small domains (or even single molecules) in monolayer films by scanning tunneling microscopy. If it is possible to record current/voltage curves on these films and discriminate between the oxidized and reduced forms of the molecules, then such materials could be a suitable medium for proving the concept of molecular data storage by redox switching.

Conclusions

Amorphous thin films of a novel series of arylamines have been prepared by vapor deposition. Film growth has been studied by AFM. Arylamine **1** initially grows as three-dimensional islands on a mica surface whereas **3** grows in a layer-by-layer mode. Spin-coating produces both crystalline and amorphous phases of **1** in thin films. Thermal annealing converts the amorphous films of **1** and **3** into crystalline phases. Cyclic voltammetry shows that the first oxidation peak observed for crystalline **1** is about 0.11 V higher than that observed for its amorphous state. CPC on 100 nm films demonstrates that the redox arrays of **2** and **3** significantly influence the efficiency of thin film oxidation of the constituent PD groups relative to that observed for the "monomeric" PD films of **1**. The unique electrochemical behaviors of these films support the notion that molecularly patterned redox arrays containing redox gradients might be useful for tuning intra- vs intermolecular charge transport in solid films and thus ultimately find applications in the design and fabrication of organic-based charge-storage memories.

Acknowledgment. We are grateful to the National Science Foundation (MRSEC award DMR-9809423) for funding this work and for supporting J.D.H. as a summer undergraduate research fellow. This work made use of the facilities supported by the Materials for Information Technology at The University of Alabama.

CM0106771